

Trustworthiness Layer for Foundation Models in Power Systems: Application for N-k Contingency Assessment

Antonio Alcántara, Spyros Chatzivasileiadis

Department of Wind and Energy Systems, Technical University of Denmark, Kgs. Lyngby, Denmark

Emails: {anmata, spchatz}@dtu.dk

Abstract—This work introduces for the first time, to our knowledge, a trustworthiness layer for foundation models in power systems. Using stratified conformal prediction, we devise adaptive, statistically valid confidence bounds for each output of a foundation model. For regression, this allows users to obtain an uncertainty estimate for each output; for screening, it supports conservative decisions that minimize false negatives. We demonstrate our method by enhancing GridFM, the first open-source Foundation Model for power systems, with statistically valid prediction intervals instead of heuristic error margins. We apply it for $N-k$ contingency assessment, a combinatorial NP-Hard problem. We show that trustworthy GridFM can offer richer and more accurate information than DC Power Flow, having 2x-3x higher precision, while running up to 18x faster than AC Power Flow for systems up to 118 buses. Moving a step further, we also examine the ability of trustworthy GridFM to generalize to unseen high-order contingencies: through a rigorous analysis, we assess how a model trained on $N-1$ or $N-2$ outages extrapolates to unseen contingencies up to $N-5$.

Index Terms—Foundation Models, Contingency Screening, Conformal Prediction, Graph Neural Networks, Power System Security

I. INTRODUCTION

The ongoing global energy transition is driving power systems toward unprecedented levels of complexity. The rapid integration of variable renewable energy sources (VRES), coupled with the electrification of heating and transport, has significantly increased the uncertainty and volatility of grid operations [1]. In this landscape, ensuring system security (specifically, the ability to withstand component failures without cascading blackouts) remains the paramount objective of Transmission System Operators (TSOs).

Conventionally, security assessment relies on *Contingency Analysis*, which entails simulating thousands of hypothetical outage scenarios (e.g., $N-1$ or $N-k$ standards) to identify potential violations [2]. While solving the full AC Power Flow (ACPF) problem provides the exact physical state for each contingency, it is still an NP-Hard problem, which is computationally prohibitive for real-time applications involving large-scale grids and massive scenario sets. As a result, industry practice often defaults to linearized DCPF approximations [3]. Although computationally efficient, DCPF relies on simplifying assumptions (unity voltage magnitudes, negligible resistances, and small angle differences) that fundamentally limits its fidelity. Crucially, DCPF neglects reactive power flows and voltage magnitude variations, rendering it incapable of detecting voltage instability or collapse, which are increasingly common drivers of blackouts in renewable-heavy grids [4].

Recently, data-driven approaches have evolved from standard regression models to topology-aware Graph Neural Net-

works (GNNs) and, most recently, to Foundation Models (FMs) for power systems [5]–[7]. Unlike traditional supervised models trained for a single specific task, FMs leverage self-supervised pre-training on massive datasets of diverse grid topologies to learn the fundamental physical laws governing power flow. By treating grid state estimation as a masked reconstruction problem (analogous to Masked Language Modeling in NLP) these models can infer complex system states orders of magnitude faster than numerical solvers.

However, the deployment of such “black-box” Artificial Intelligence (AI) in safety-critical infrastructure faces two major hurdles: *trustworthiness* and *generalization*. First, operators cannot rely on a model that provides point predictions without valid uncertainty estimates; a model that *hallucinates* a physically consistent but incorrect safe state during a contingency could lead to catastrophic failure. Second, statistical models struggle with distributional shifts. A model trained primarily on routine single-line outages ($N-1$) must reliably extrapolate to rarer, high-impact multi-component failures ($N-k$) without requiring exhaustive retraining: a capability that remains an open challenge in current research [8].

The main contribution of this work is the development of a trustworthy contingency screening framework by enhancing the physics-informed GridFM [5] with a Stratified Conformal Prediction layer. By replacing heuristic error margins with mathematically guaranteed coverage [9], [10], we construct statistically valid uncertainty intervals for voltages and line loadings that effectively minimize false negatives. Beyond ensuring safe operation, we demonstrate the model’s ability to reconstruct full AC system states and validate its robustness through a rigorous generalization analysis, specifically assessing performance on unseen, high-severity contingencies (up to $N-5$) when trained only on routine outages.

II. BACKGROUND AND RELATED WORK

A. Foundation Models for Power Systems

FMs represent a paradigm shift in AI, characterized by advanced deep learning architectures pre-trained on massive, diverse datasets through self-supervision to autonomously extract structural information and rich representations of complex systems [5] [11]. Unlike traditional machine learning (ML) models that are typically task-specific, FMs utilize Transformer architectures and large-scale compute resources to achieve high generalization, enabling efficient adaptation to various downstream applications with minimal labeled data. In the context of the electric power grid, these models are emerging as novel tools capable of redefining how complexity and uncertainty are managed in the context of the global energy transition.

In addition to versatility and flexibility, one of the most salient advantages of the FM approach is its potential to close the widening computational gap in grid operations. This gap is driven by a system with increasingly fast dynamics and complexity that effectively outpaces modern computational hardware. By providing significant speed-ups over traditional iterative physics-based solvers, the FM approach offers a scalable solution where current tools fall short. Recent conceptual frameworks, such as *GridFM* [5], demonstrate the use of Graph Neural Networks (GNNs) in combination with Transformers to learn the fundamental physics of ACPF in a self-supervised manner. Furthermore, specialized FMs like *PowerPM* [12] have been designed to simultaneously capture the intricate temporal dependencies and hierarchical structures inherent in electricity time series (ETS) data, significantly improving performance in tasks ranging from demand-side forecasting to grid stability monitoring.

The application of Large Language Models (LLMs) has also expanded into the energy sector to handle unstructured data, including knowledge retrieval from technical documents, code generation for power system simulation, and serving as iterative optimizers for problems like Optimal Power Flow (OPF) and electric vehicle scheduling [7] [13]. Comprehensive initiatives like NREL's *eGridGPT* emphasize the role of AI orchestration and digital twins to integrate these models with existing control rooms, ensuring that AI-driven insights are validated against real-world grid conditions [14]. However, the integration of FMs into critical infrastructure requires addressing significant hurdles, including data privacy, cybersecurity vulnerabilities, and the risk of *hallucinations*, encouraging the development of robust frameworks that ensure that forecasted outputs do not cause catastrophic oversights in the operation of real-world power systems.

B. Machine Learning for Contingency Analysis

While FMs aim for flexibility and generalization in power systems, the specific task of contingency analysis (assessing the grid's security under hypothetical component outages) has spurred the development of specialized ML architectures. Traditional physics-based solvers, such as the Newton-Raphson method for ACPF, often become computationally prohibitive as the combinatorial space of $N-k$ scenarios grows, particularly for large-scale systems [6]. Consequently, recent research has shifted toward Graph Neural Networks (GNNs) and reinforcement learning to provide rapid, topology-aware security assessments [6] [15] [16].

GNNs have emerged as a dominant architecture due to their ability to inherently exploit the structural characteristics of the power grid, enabling the model to process both node-level (bus) and edge-level (transmission line) information. For instance, GNN-based frameworks have been successfully applied to fast contingency screening, demonstrating the capability to generalize from $N-1$ training scenarios to unseen $N-2$ and $N-3$ topologies with a speedup of up to 400 times compared to traditional solvers [6]. Such models effectively bypass the need for exhaustive iterative numerical simulations by learning to approximate the physical state of the grid directly from its topological representation [6] [17].

Beyond steady-state estimation, ML is increasingly utilized for dynamic security and multi-stability risk assessment. Specialized GNN architectures can simultaneously predict multiple stability types, including rotor angle, voltage, and frequency stability, enabling real-time risk visualization through non-convex alpha shapes [15]. In the context of preventive control, GNNs serve as highly efficient surrogates for Transient Security Assessment (TSA), allowing for the rapid solution of security-constrained optimal power flow (TSC-OPF) problems that were previously limited by the intensity of solving differential-algebraic equations [17].

Furthermore, multi-agent deep reinforcement learning has been proposed to manage the high uncertainties inherent in post-contingency dynamic operations, such as varying fault durations and load consumption [16]. By integrating graph-attention mechanisms with GCN-powered agents, these models can capture complex spatiotemporal features and facilitate cooperative learning among different grid sub-networks.

C. Uncertainty Quantification

As power systems transition toward high renewable penetration, the level of operational uncertainty (stemming from stochastic generation and complex $N-k$ fault scenarios) has increased significantly. In such safety-critical infrastructure, relying on deterministic point predictions from ML models is insufficient, as *hallucinations* or minor estimation errors can lead to catastrophic operational oversights, cascading failures, or total voltage collapse. Therefore, measuring the reliability of AI-driven insights is paramount to ensure that they can be validated against real-world grid conditions [18].

Conformal Prediction (CP) has recently emerged as a leading framework for Uncertainty Quantification (UQ) because it provides statistically rigorous guarantees without requiring restrictive distributional assumptions about the data [19]. Originally rooted in Kolmogorov's notion of randomness, CP delivers exact prediction intervals for future observations that are guaranteed to contain the ground truth with a user-specified probability level [9]. This makes it a generalizable and easy-to-implement bridge for reliable AI, particularly in domains where data may be non-Gaussian or subject to dynamic temporal dependencies [20].

In the context of contingency analysis, this framework could be applied to calibrate the FM regression outputs (such as bus voltages and line loadings) into prediction intervals. By defining a non-conformity score based on derived physical quantities, CP could effectively create a "safety interval" for congestion screening. Such an approach would add a layer of *statistical robustness*, significantly reducing the risk of false negatives by ensuring that contingencies leading to potential operational violations are not incorrectly classified as safe.

III. PROBLEM FORMULATION

We formulate the problem of contingency analysis as a data-driven state estimation task. While traditionally treated as a set of independent numerical solutions (ACPF) for each topology, we approach it as learning a continuous function over the manifold of grid topologies. Formally, this involves two stages:

first, utilizing a FM to infer the high-dimensional physical state (voltage magnitudes and angles) from the network topology; and second, deriving physics-consistent line flows to screen for operational violations.

A. State Prediction

Let $\mathcal{G} = (\mathcal{N}, \mathcal{E})$ represent the power grid graph, where \mathcal{N} is the set of buses and \mathcal{E} is the set of transmission lines and transformers. An operating point under a contingency k is defined by the input feature vector x_k , which encompasses the network topology (identifying the outaged component), the active and reactive power injections at all buses, and the generator voltage setpoints.

The fundamental physical state of the system is defined by the complex voltage at every bus $i \in \mathcal{N}$. We denote the target state vector as $y = [|V|, \theta] \in \mathbb{R}^{2|\mathcal{N}|}$, where $|V|$ represents the voltage magnitudes and θ represents the voltage angles. This ground truth y is obtained by solving the ACOPF equations [21], a system of non-linear algebraic equations that enforce Kirchhoff's laws and power balance constraints. While ACOPF provides the exact physical solution, its iterative numerical solution (typically via Newton-Raphson) is computationally intensive for large-scale contingency screening.

Consequently, we define the learning task as training/fine-tuning a parameterized function f_ϕ (the FM) that approximates this non-linear mapping from the contingency input to the system state:

$$\hat{y} = [|\hat{V}|, \hat{\theta}] = f_\phi(x_k) \quad (1)$$

where \hat{y} is the predicted state vector intended to estimate the ACOPF solution.

B. Physics-Consistent Line Flow Calculation

We adopt a physics-consistent approach based on the π -equivalent transmission line model. The loading is determined by the current magnitudes flowing at both the “from” (f) and “to” (t) ends of the branch. Let $Y_f, Y_t \in \mathbb{C}^{|\mathcal{E}| \times |\mathcal{N}|}$ be the system branch admittance matrices mapping bus voltages to branch currents at the respective ends, accounting for both series impedance and shunt admittances.

First, we reconstruct the vector of complex bus voltages $\hat{\mathbf{V}} \in \mathbb{C}^{|\mathcal{N}|}$ from the predicted magnitudes and angles, such that the i -th element is $\hat{V}_i = |\hat{V}|_i e^{j\hat{\theta}_i}$. The complex current vectors $I_f, I_t \in \mathbb{C}^{|\mathcal{E}|}$ are then computed as:

$$I_f = Y_f \hat{\mathbf{V}}, \quad I_t = Y_t \hat{\mathbf{V}} \quad (2)$$

C. Congestion Screening

One of the downstream tasks of interest is Congestion Screening: a binary classification problem that determines if a specific contingency leads to operational violations. The screening task involves identifying thermal violations. For a line l , the thermal rating is given as $S_{rated}^{(l)}$ (MVA). We convert this to a current limit $I_{limit}^{(l)}$ based on the line-to-line base voltage $V_{base}^{(l)}$:

$$I_{limit}^{(l)} = \frac{S_{rated}^{(l)}}{\sqrt{3} \cdot V_{base}^{(l)}} \quad (3)$$

The line loading ratio L_l is defined as the maximum utilization at either end of the line:

$$L_l = \max \left(\frac{|I_{f,l}|}{I_{limit}^{(l)}}, \frac{|I_{t,l}|}{I_{limit}^{(l)}} \right) \quad (4)$$

The binary classification target (Safe/Unsafe) for a line l is determined by whether $L_l > 1.0$.

D. The Standard Approach: DC Power Flow

In industrial practice, where thousands of potential contingencies ($N-1, N-k$) must be evaluated rapidly, solving the full non-linear ACOPF for every scenario is computationally prohibitive. Consequently, the industry standard for contingency screening is the DC Power Flow (DCPF).

DCPF linearizes the AC equations based on three simplifying assumptions: Voltage magnitudes are fixed at unity ($|V_i| \approx 1.0$ p.u.); branch resistances are negligible compared to reactances ($R \ll X$); and voltage angle differences across lines are small ($\sin(\theta_i - \theta_j) \approx \theta_i - \theta_j$) [3].

Under these assumptions, the power flow problem reduces to a linear system of equations $P = B_{bus}\theta$, where P is the vector of active power injections and B_{bus} is the DC system susceptibility matrix. This system can be solved orders of magnitude faster than ACOPF. However, this efficiency comes at the cost of fidelity: DCPF completely neglects reactive power flows and voltage magnitude variations. As a result, it is incapable of detecting voltage violations (over/under-voltages) and often incurs significant errors in line flow estimates under stressed grid conditions.

IV. METHODOLOGY: CALIBRATED AND RELIABLE FOUNDATION MODELS

To address the challenge of real-time contingency screening defined in Section III, we leverage the GridFM framework [5], a pre-trained foundation model designed to capture the non-Euclidean topology of power systems. We focus on analyzing the generalization capabilities of GridFM when applied to safety-critical contingency analysis. Our methodology consists of three distinct pillars: first, the adaptation of the GridFM backbone (Section IV-A); second, a physics-informed fine-tuning strategy that forces the model to learn the underlying AC state (Section IV-B); and third, a rigorous uncertainty quantification layer using Stratified CP to ensure reliability (Section IV-C).

A. The GridFM Architecture

We employ the GridFM architecture [5], a specialized Graph Transformer designed to process the heterogeneous and non-Euclidean structure of power grids. Unlike standard Transformers that treat data as sequential tokens, GridFM operates directly on the graph topology $\mathcal{G} = (\mathcal{N}, \mathcal{E})$. Here, \mathcal{N} represents the buses and \mathcal{E} represents the set of branches

(transmission lines l), ensuring the model respects the physical connectivity of the grid.

The architecture follows an encoder-decoder structure. The encoder processes the network topology and known injection values using Multi-Head Graph Attention layers. For every bus i , the model maintains a latent feature vector $h_i^{(\tau)} \in \mathbb{R}^d$ at layer τ , where the initial state $h_i^{(0)}$ represents the input node features (e.g., active power injection, voltage setpoint).

For a given layer, the attention mechanism aggregates features from connected neighbors $j \in \mathcal{N}(i)$, where the connectivity is strictly defined by the branches $l = (i, j) \in \mathcal{E}$. The aggregation is weighted by learned coefficients α_{ij} that capture the strength of physical coupling. To capture different types of interactions, the model employs H independent attention heads. The update rule for the feature vector at layer $\tau + 1$ is:

$$h_i^{(\tau+1)} = \text{Concat}_{m=1}^H \left[\sum_{j \in \mathcal{N}(i)} \alpha_{ij,m}^{(\tau)} W_m^{(\tau)} h_j^{(\tau)} \right] \quad (5)$$

where m indexes the attention head, $W_m^{(\tau)}$ are trainable weight matrices, and $\alpha_{ij,m}^{(\tau)}$ is the attention score. This mechanism allows the model to propagate information across the branches, effectively learning the long-range dependencies inherent in Kirchhoff's laws. By encoding the explicit topology in the message-passing steps, the architecture is naturally flexible to the structural changes required for contingency analysis (i.e., the removal of a line l_{out}).

B. Fine-tuning Strategy

To adapt the pre-trained FM for rigorous contingency screening, we frame the task as a state reconstruction problem rather than a direct binary classification of line overflows. This design choice ensures that the model's outputs remain physics-consistent and interpretable.

We utilize a partial masking strategy to simulate the contingency solving process. For a specific contingency sample k (corresponding to the outage of branch(es) l_{out}), the graph structure is modified by removing the edge(s) corresponding to l_{out} . Then, the known variables (generator voltage magnitudes, active power setpoints, and load demands) are provided as input features X_{input} , and the target state variables (load bus voltage magnitudes $|V|$ and all voltage angles θ) are masked with a learnable token.

The model is fine-tuned for the reconstruction of masked physical states, effectively learning the underlying ACPF solution. This contrasts with direct classification, which suffers from significant information loss by abstracting the continuous state into a binary label. By retaining the continuous physical variables, a single model is able to screen for diverse constraint violations, covering both voltage magnitudes and line thermal limits. The loss function \mathcal{L} is defined as the Mean Squared Error (MSE) between the predicted state vectors and the ground truth values obtained from the Newton-Raphson solver:

$$\mathcal{L} = \frac{1}{|\mathcal{N}_{mask}|} \sum_{i \in \mathcal{N}_{mask}} \left[\left(|V|_i - |\hat{V}|_i \right)^2 + \left(\theta_i - \hat{\theta}_i \right)^2 \right] \quad (6)$$

where \mathcal{N}_{mask} represents the set of nodes with masked state variables. By focusing on minimizing the error in V and θ , we ensure that the subsequent calculation of line flows (as detailed in Section III-B) is derived from a coherent system state, reducing the risk of hallucinating physically impossible flow patterns.

C. Bounding with Conformal Prediction

To deploy a FM in a safety-critical environment, point predictions must be accompanied by rigorous uncertainty quantification. We employ Split CP [9] to construct statistically valid prediction intervals that contain the ground truth with a user-specified probability $1 - \alpha$.

1) *General Formulation*: Consider a calibration dataset $\mathcal{D}_{cal} = \{(x_j, y_j)\}_{j=1}^M$ that is exchangeable with the test data. We first compute a non-conformity score s_j that measures the disagreement between the model's prediction \hat{y}_j and the true value y_j . A standard choice for regression tasks is the absolute residual:

$$s_j = |y_j - \hat{y}_j| \quad (7)$$

We then compute \hat{q} , the $\lceil (M + 1)(1 - \alpha) \rceil / M$ -th empirical quantile of the scores $\{s_1, \dots, s_M\}$. For a new input x_{new} , the prediction interval $\mathcal{C}(x_{new})$ is given by:

$$\mathcal{C}(x_{new}) = [\hat{y}_{new} - \hat{q}, \hat{y}_{new} + \hat{q}] \quad (8)$$

By definition, this interval guarantees marginal coverage: $\mathbb{P}(y_{new} \in \mathcal{C}(x_{new})) \geq 1 - \alpha$.

2) *Application to Contingency Screening*: In the context of contingency screening, we apply this calibration to the physical variables of interest: voltage magnitudes $|V|$ and line loading ratios L . The computed quantile \hat{q} acts as a robust safety interval. For example, regarding voltage security, we compute a specific quantile \hat{q}_V . A bus i is flagged as potentially unsafe not merely if its predicted voltage $|\hat{V}|_i$ exceeds the limit V_{max} , but if the *upper bound* of its prediction interval violates the limit:

$$|\hat{V}|_i + \hat{q}_V > V_{max} \quad (9)$$

Similarly, for line overloading, we utilize the upper bound of the loading prediction $\hat{L}_l + \hat{q}_L$ to detect violations conservatively, minimizing the false negative rate (missed alarms). If only the upper bound is operationally relevant (as in line-loading screening), the conformalization can be restricted to a one-sided (upper-tail) interval by selecting the corresponding one-sided quantile, thereby avoiding unnecessary widening of the lower bound.

3) *Stratified Calibration for Contingency Levels*: Standard CP assumes that test data is drawn from the same distribution as the calibration data. However, in contingency analysis, this assumption is challenged by the severity of the outage. A model trained primarily on single-component outages ($N-1$) typically exhibits higher predictive errors when evaluated on more complex, unseen topologies ($N-k$, where $k > 1$). Consequently, utilizing a trivial, global non-conformity score would result in under-coverage for severe contingencies and unnecessarily wide intervals for simple ones.

To address this, we propose a Stratified CP approach. We partition the calibration set into subsets based on the contingency level k and the specific element index (bus i or line l). We pre-compute validation scores specifically for these groups, allowing the prediction interval to adapt to the local volatility of specific grid components.

For a target bus i and a target line l under a contingency of level k , we construct the prediction intervals using specific quantiles $\hat{q}_{V,(i,k)}$ and $\hat{q}_{L,(l,k)}$, derived from the residuals of that specific element across the available $N-k$ calibration samples:

$$\mathcal{C}_{i,k}^V = |\hat{V}|_i \pm \hat{q}_{V,(i,k)}, \quad \mathcal{C}_{l,k}^L = \hat{L}_l \pm \hat{q}_{L,(l,k)} \quad (10)$$

By defining element-wise and level-specific quantiles, the screening mechanism provides tighter bounds for stable components while automatically expanding the safety margin for lines or buses that are historically difficult to model under high-stress $N-k$ conditions.

V. NUMERICAL RESULTS AND DISCUSSION

In this section, we evaluate the performance of the GridFM framework on the IEEE 24-bus and IEEE 118-bus systems. Our analysis focuses on three key dimensions: the fidelity of AC state reconstruction under unseen topologies, the classification performance for congestion screening, and the enhancement of trustworthiness through CP.

A. Experimental Setup

The experiments were conducted in a High Performance Computing (HPC) cluster, using an NVIDIA V100 GPU equipped with 16GB of memory for model fine-tuning. Dataset and benchmark generation tasks including AC and DCPF solving were executed on a 16-core Intel Xeon 6226R processor with 256 GB of RAM.

To assess generalization capabilities, we utilized the *GridFM-datakit* [22] to generate datasets characterized by varying contingency distributions. As summarized in Table IV (see Appendix), we established three distinct training configurations: Set A (restricted to $N-1$ outages), Set B (a mixture of $N-1$ and $N-2$), and Set C (uniform distribution from $N-1$ to $N-5$).

Evaluation is performed on a held-out test set containing a uniform distribution of unseen contingencies ($N-1$ to $N-5$). This set comprises 150,000 and 200,000 samples for the IEEE 24-bus and IEEE 118-bus systems, respectively.

B. State Estimation Performance

We first analyze the model's ability to reconstruct the system state (Voltage Magnitudes $|V|$ and Angles θ). The fidelity of these estimates is critical, as they form the basis for detecting violations. Tables I and II present the estimation errors.

A clear difference is observed in the generalization capabilities of the models. In the IEEE-24 system, the sharp degradation of GridFM-A as k increases is consistent with a train/test shift: Set A is trained exclusively on $N-1$, whereas the test distribution includes higher-order contingencies, making extrapolation errors grow with severity (MAE

TABLE I
GRIDFM VOLTAGE MAGNITUDE ESTIMATION ERROR UNDER DIFFERENT FINE-TUNING APPROACHES (MAE IN P.U.)

	IEEE 24-bus			IEEE 118-bus		
	A (N-1)	B (N-1/2)	C (Unif. N-1...5)	A (N-1)	B (N-1/2)	C (Unif. N-1...5)
$N-1$	0.0029	0.0031	0.0009	0.0017	0.0009	0.0013
$N-2$	0.0035	0.0035	0.0010	0.0017	0.0010	0.0013
$N-3$	0.0047	0.0040	0.0012	0.0018	0.0011	0.0014
$N-4$	0.0062	0.0048	0.0016	0.0019	0.0011	0.0013
$N-5$	0.0084	0.0059	0.0022	0.0020	0.0012	0.0014
Overall	0.0054	0.0044	0.0014	0.0018	0.0010	0.0013

TABLE II
GRIDFM VOLTAGE ANGLE ESTIMATION ERROR UNDER DIFFERENT FINE-TUNING APPROACHES (MAE IN DEGREES)

	IEEE 24-bus			IEEE 118-bus		
	A (N-1)	B (N-1/2)	C (Unif. N-1...5)	A (N-1)	B (N-1/2)	C (Unif. N-1...5)
$N-1$	1.58	1.08	0.53	3.19	2.71	4.03
$N-2$	2.15	1.25	0.62	3.28	2.72	4.06
$N-3$	3.21	1.58	0.74	3.49	3.20	4.63
$N-4$	4.64	2.32	1.01	3.49	2.90	4.10
$N-5$	5.99	2.97	1.29	3.94	3.46	4.66
Overall	3.72	1.92	0.87	3.46	2.97	4.28

triples from $N-1$ to $N-5$ on both voltage magnitude and angle estimation). On the contrary, GridFM-C demonstrates superior stability, achieving the lowest overall MAE for both voltage magnitude and angle, validating the benefit of uniform training distributions for smaller, highly sensitive networks.

On IEEE-118, GridFM-B ($N-1/N-2$ mixture) attains the lowest MAE (0.001,p.u. for voltage magnitudes and 2.97° for angles). This result highlights a critical trade-off between training resources and system complexity. In the smaller IEEE-24, where representational resources are high relative to the system size, the model benefits from the broad coverage of a uniform distribution (GridFM-C). In contrast, given the finite data resources available relative to the expanded IEEE-118 state space (see Table IV in the Appendix), we observe that focusing on $N-1$ and $N-2$ contingencies yields more efficient learning. This suggests that attempting to cover the vast combinatorial space of $N-5$ outages in large systems can dilute model performance, making a concentrated training strategy superior when data are limited.

C. Congestion Screening Capabilities

Accurate state estimation allows for direct detection of thermal overloads. In this section, we compare the screening performance of the proposed models against the industry-standard DCPF baseline, distinguishing performance primarily through Recall (Sensitivity). We also report Precision to quantify selectivity, using the format *recall* (*precision*).

Recall is defined as True Positives/(True Positives + False Negatives), representing the fraction of actual violations that are successfully detected by the model. In the context of contingency screening, this is the most critical metric because the cost of errors is asymmetric: a “False Negative” (missing a dangerous violation) poses a severe security risk that can lead to cascading failures, whereas a “False Positive” (flagging a safe scenario as dangerous) merely incurs the computational cost of running a verification check. Therefore, achieving a

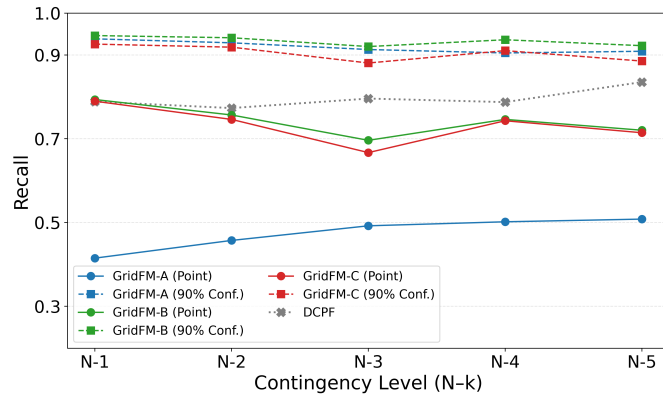


Fig. 1. Recall for line congestion screening under different contingency levels on IEEE-118 system. Results for the different GridFM models, with and without conformalization.

recall near 1.0 is a non-negotiable requirement for reliability; precision complements recall by indicating how many of the flagged cases are truly critical.

Table VI (see Appendix for full details) reveals the distinct behaviors between the two systems. In the IEEE 24-bus system, GridFM-C (trained on uniform severities) is the model that consistently outperforms the DCPF baseline, achieving an overall *recall* (*precision*) of 0.902 (0.736) compared to 0.722 (0.477) for DCPF. Notably, models trained on narrower distributions fail to generalize significantly, with GridFM-A reaching only 0.199 (0.071) overall, and GridFM-B 0.488 (0.473). This highlights that for smaller, constrained networks, exposure to the full range of $N-k$ topologies during fine-tuning is necessary for accurate screening and acceptable selectivity.

In the IEEE 118-bus system, the DCPF baseline attains an overall 0.801 (0.102), marginally surpassing the raw point estimates of GridFM-B 0.736 (0.537) and GridFM-C 0.726 (0.360). However, this performance must be contextualized by selectivity: DCPF's higher recall is largely an artifact of over-conservative linear approximations that flag a large number of safe states as risky, as reflected in its precision near 0.10. In contrast, at similar recall levels, the GridFM models provide 3x-5x precision gains (e.g., 0.537 for Set B and 0.360 for Set C), indicating better discrimination and fewer unnecessary follow-up checks.

D. Increasing Reliability with Conformal Prediction

To bridge the reliability gap observed in the raw regression outputs, we implemented the Stratified CP framework detailed in Section IV-C, focusing on the upper bound. This process leverages a dedicated calibration dataset comprising approximately 20,000 samples, stratified across varying contingency severities. This dataset serves to empirically estimate the distribution of non-conformity scores, enabling the computation of adaptive quantiles $\hat{q}_{L,(l,k)}$ to be used on test data.

For the sake of brevity, we focus on the IEEE-118. Fig. 1 and Table VII (Appendix) show that calibration markedly increases the recall up to more than 0.90 across all $N-k$ levels for all GridFM variants. In terms of overall performance, calibration lifts GridFM to 0.915 (0.206) for Set A, 0.931

TABLE III
COMPUTATIONAL PERFORMANCE (TIME IN MS PER SCENARIO)

Method	Hardware	IEEE-24	IEEE-118
ACPF	CPU	1.60	6.73
DCPF	CPU	0.62	0.59
GridFM (Inf.)	GPU	0.34	0.36

(0.325) for Set B, and 0.901 (0.283) for Set C, clearly surpassing the DCPF baseline 0.801 (0.102). Results for IEEE-24 are also detailed on Table VII (Appendix).

Inherently, introducing a safety interval to maximize recall incurs a trade-off in selectivity, leading to a naturally higher rate of False Positives. This precision-recall dynamic on IEEE-118 is presented in Fig. 2 (see Appendix). Notably, even after calibration, the GridFM-B maintain precision gains higher than 3x compared to the DCPF baseline, demonstrating that the safety gains do not come at the cost of excessive conservatism.

E. Computational Efficiency Analysis

We assess the computational feasibility of the proposed framework by comparing end-to-end *inference* latency per scenario against Julia-based AC and DC solvers from the *GridFM-datakit* [22]. GridFM timings are measured with batched inference on a single GPU. ACPF and DCPF run on CPU with parallel execution across all available cores.

Because GridFM uses the same fixed, weight-shared architecture across networks, its per-scenario inference on GPU remains near-constant, showing only a negligible change from IEEE-24 (0.34 ms) to IEEE-118 (0.36 ms), i.e., runtime does not scale appreciably with system size (Table III). Against ACPF on CPU, this yields an $\sim 18\times$ speedup on the 118-bus case (6.73 ms \rightarrow 0.36 ms). Moreover, GridFM inference is competitive with, and effectively faster than, DCPF on CPU (0.59 ms) while returning the full AC state (voltages and angles). These results indicate that GridFM is suitable for strict real-time requirements in online contingency analysis, especially for larger systems.

Fine-tuning times are reported in Table V from the Appendix: for 100 epochs they range from 30 to 83 minutes on IEEE-24 and from 123 to 145 minutes on IEEE-118.

VI. CONCLUSION

This work introduces a trustworthiness layer for FMs, deployed on GridFM, using stratified conformal prediction that converts point forecasts into statistically guaranteed, risk-controllable bounds for voltages and line loadings. On IEEE 24- and 118-bus systems, this layer preserves AC fidelity while raising recall above 0.9 across $N-k$ levels and significantly surpassing DCPF with higher precision. Topological diversity during fine-tuning is crucial: mixed-severity training generalizes to unseen higher-order outages, whereas $N-1$ -only training fails to extrapolate. Inference is real-time (around 0.36ms per scenario on GPU with near size-invariant latency) and returns the full AC state, yielding up to 18x speedup over ACPF and 2x-3x precision gains vs. DCPF for screening. Future work will address richer calibration by topology and

operating regime and scaling to larger grids while tightening the coverage–precision trade-off under distribution shift.

VII. AI USAGE DISCLOSURE

Microsoft Copilot and Claude Opus were used for writing assistance (copy-editing) and to generate code related to plotting/formatting. All scientific content and results were produced by the authors.

APPENDIX

A. Dataset Construction and Fine-Tuning Runtime

This appendix documents the composition of the fine-tuning datasets and the wall-clock training time used to produce the GridFM models evaluated in the main paper. Table IV summarizes, for each system and split (*Set A/B/C*), the number of operating conditions, the maximum number of topologies synthesized, the contingency sampling scheme, and the total number of generated samples. In our setting, an individual sample corresponds to a single scenario defined by (i) an operating condition (load/generation realization), (ii) a network topology within the specified limit, and (iii) a contingency drawn according to the indicated $N-k$ scope.

TABLE IV
DATASET COMPOSITION AND GENERATION PARAMETERS

System	Set	Op. Cond.	Max Topologies	Contingency Scope	Samples
IEEE-24	A	1000	100	Only $N-1$	38,000
	B	500	200	Prob $N-k$ [0.2, 0.8]	99,941
	C	500	200	Uniform $N-k$	97,748
IEEE-118	A	500	200	Only $N-1$	88,992
	B	500	200	Prob $N-k$ [0.2, 0.8]	100,000
	C	500	200	Uniform $N-k$	100,000

Unless otherwise noted, each model is fine-tuned for 100 epochs with an 80/20 train/validation split (no held-out test set during fine-tuning). Batch size and early-stopping patience (when enabled) are reported explicitly in Table V. The reported times are end-to-end wall-clock training durations and the corresponding average time per epoch. Because each synthetic scenario requires a single ACDF solution, the total data-generation time grows essentially linearly with dataset size; a good rule of thumb is $T_{\text{gen}} \approx N_{\text{samples}} \cdot t_{\text{ACDF}}$, with only small constant overheads for I/O, infeasibility checks, and logging.

TABLE V
FINE-TUNING TIME PER DATASET SPLIT (100 EPOCHS)

Case	Set	Batch	Patience	Train Time (s)	Time/Epoch (s)
IEEE-24	A	128	25	1816.45	18.16
	B	128	25	5008.92	50.09
	C	128	25	4732.40	47.32
IEEE-118	A	256	20	7351.01	73.51
	B	256	20	8724.31	87.24
	C	256	20	8374.41	83.74

B. Extended Results on Congestion Screening

This appendix complements the main text by reporting per- $N-k$ recall for line-congestion screening across training splits (GridFM-A/B/C) and systems (IEEE-24/118), both for

point predictions and for CPs at 90% coverage using our stratified conformal procedure.

For each $N-k$ level, the value is the fraction of truly congested lines correctly flagged (recall). The *Overall* row aggregates across all contingency levels and scenarios. Table VI lists the point-estimate recalls; Table VII shows the recalls after conformal calibration (target coverage 90%). Fig. 2 summarizes the precision–recall trade-off for the overall metrics.

As can be noticed, conformal calibration reliably raises recall toward the target across all $N-k$ levels and both systems, with the largest gains for GridFM-A (the least stress-exposed training split) and consistently high recall for GridFM-C. As expected, higher recall under calibration comes with lower precision (see Fig. 2), yet the calibrated models still higher precision compared to DCPF.

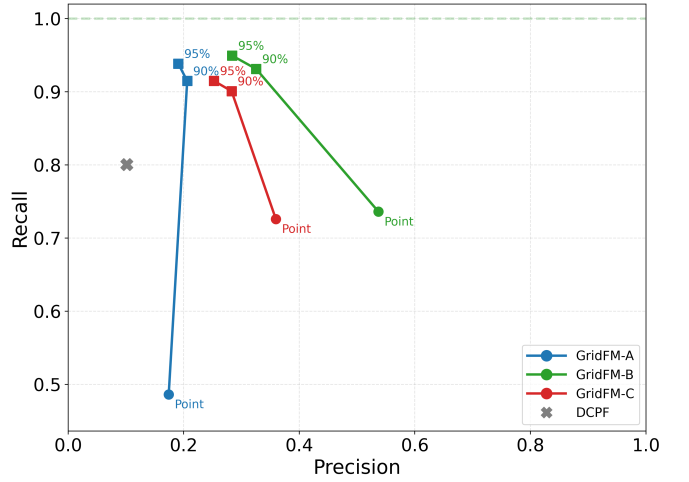


Fig. 2. Precision–Recall trade-off for GridFM on the IEEE-118 system (overall metrics). Dots indicate point estimates; squares indicate 90%/95% conformal settings; the gray cross is the DCPF baseline. Lines connect each model family across settings.

REFERENCES

- [1] M. S. Alam, F. S. Al-Ismail, A. Salem, and M. A. Abido, “High-level penetration of renewable energy sources into grid utility: Challenges and solutions,” *IEEE access*, vol. 8, pp. 190 277–190 299, 2020.
- [2] A. J. Wood, B. F. Wollenberg, and G. B. Sheblé, *Power generation, operation, and control*. John wiley & sons, 2013.
- [3] B. Stott, J. Jardim, and O. Alsaç, “Dc power flow revisited,” *IEEE Transactions on Power Systems*, vol. 24, no. 3, pp. 1290–1300, 2009.
- [4] Y. G. Werkie, G. N. Nyakoe, and C. W. Wekesa, “Power system voltage stability assessment and control strategies: State-of-the-art review,” *Journal of Electrical and Computer Engineering*, vol. 2025, no. 1, p. 6667482, 2025.
- [5] H. F. Hamann, B. Gjorgiev, T. Brunschwiler, L. S. Martins, A. Puech, A. Varbella, J. Weiss, J. Bernabe-Moreno, A. B. Massé, S. L. Choi *et al.*, “Foundation models for the electric power grid,” *Joule*, vol. 8, no. 12, pp. 3245–3258, 2024.
- [6] A. M. Nakiganda and S. Chatzivasileiadis, “Topology-aware neural networks for fast contingency analysis of power systems,” *arXiv preprint arXiv:2310.04213*, 2023.
- [7] C. Huang, S. Li, R. Liu, H. Wang, and Y. Chen, “Large foundation models for power systems,” in *2024 IEEE Power & Energy Society General Meeting (PESGM)*. IEEE, 2024, pp. 1–5.
- [8] S. Yang, B. Vaagensmith, and D. Patra, “Power grid contingency analysis with machine learning: A brief survey and prospects,” *2020 Resilience Week (RWS)*, pp. 119–125, 2020.

TABLE VI

GRIDFM RECALL (PRECISION) FOR LINE CONGESTION SCREENING UNDER DIFFERENT FINE-TUNING APPROACHES (POINT ESTIMATES, DCPF AS BASELINE)

IEEE 24-bus				IEEE 118-bus				
	A (N-1)	B (N-1/2)	C (Unif. N-1...5)	DCPF	A (N-1)	B (N-1/2)	C (Unif. N-1...5)	DCPF
N-1	0.462 (0.034)	0.512 (0.249)	0.985 (0.575)	0.632 (0.170)	0.415 (0.088)	0.794 (0.476)	0.790 (0.250)	0.789 (0.048)
N-2	0.267 (0.043)	0.477 (0.355)	0.981 (0.689)	0.621 (0.281)	0.457 (0.137)	0.757 (0.542)	0.746 (0.309)	0.773 (0.072)
N-3	0.236 (0.064)	0.554 (0.452)	0.907 (0.703)	0.767 (0.423)	0.492 (0.163)	0.696 (0.491)	0.667 (0.312)	0.796 (0.096)
N-4	0.223 (0.100)	0.544 (0.521)	0.905 (0.749)	0.762 (0.521)	0.502 (0.231)	0.746 (0.586)	0.743 (0.450)	0.788 (0.140)
N-5	0.136 (0.084)	0.418 (0.509)	0.878 (0.766)	0.697 (0.602)	0.508 (0.223)	0.720 (0.547)	0.714 (0.425)	0.835 (0.160)
Overall	0.199 (0.071)	0.488 (0.473)	0.902 (0.736)	0.722 (0.477)	0.486 (0.174)	0.736 (0.537)	0.726 (0.360)	0.801 (0.102)

TABLE VII

GRIDFM RECALL (PRECISION) FOR LINE CONGESTION SCREENING UNDER DIFFERENT FINE-TUNING APPROACHES (CONFORMAL PREDICTION AT 90% COVERAGE FOR GRIDFM, DCPF AS BASELINE)

IEEE 24-bus				IEEE 118-bus				
	A (N-1)	B (N-1/2)	C (Unif. N-1...5)	DCPF	A (N-1)	B (N-1/2)	C (Unif. N-1...5)	DCPF
N-1	0.940 (0.058)	0.992 (0.250)	0.995 (0.537)	0.632 (0.170)	0.939 (0.129)	0.946 (0.212)	0.926 (0.160)	0.789 (0.048)
N-2	0.728 (0.090)	0.983 (0.378)	0.993 (0.635)	0.621 (0.281)	0.929 (0.176)	0.941 (0.286)	0.919 (0.230)	0.773 (0.072)
N-3	0.579 (0.118)	0.927 (0.418)	0.980 (0.632)	0.767 (0.423)	0.913 (0.192)	0.920 (0.305)	0.881 (0.265)	0.796 (0.096)
N-4	0.521 (0.157)	0.907 (0.431)	0.960 (0.659)	0.762 (0.521)	0.905 (0.257)	0.936 (0.388)	0.910 (0.370)	0.788 (0.140)
N-5	0.430 (0.168)	0.868 (0.431)	0.957 (0.620)	0.697 (0.602)	0.909 (0.248)	0.922 (0.385)	0.886 (0.362)	0.835 (0.160)
Overall	0.521 (0.131)	0.903 (0.416)	0.966 (0.633)	0.722 (0.477)	0.915 (0.206)	0.931 (0.325)	0.901 (0.283)	0.801 (0.102)

- [9] V. Vovk, A. Gammerman, and G. Shafer, *Algorithmic learning in a random world*. Springer, 2005.
- [10] A. Bellotti and X. Zhao, “Conformal prediction and trustworthy ai,” *arXiv preprint arXiv:2508.06885*, 2025.
- [11] G. Antonesi, T. Cioara, I. Anghel, V. Michalakopoulos, E. Sarmas, and L. Toderean, “From transformers to large language models: A systematic review of ai applications in the energy sector towards agentic digital twins,” *arXiv preprint arXiv:2506.06359*, 2025.
- [12] S. Tu, Y. Zhang, J. Zhang, Z. Fu, Y. Zhang, and Y. Yang, “Powerpm: Foundation model for power systems,” *Advances in Neural Information Processing Systems*, vol. 37, pp. 115 233–115 260, 2024.
- [13] H. Mirshekali, M. R. Shadi, F. G. Ladani, and H. R. Shaker, “A review of large language models for energy systems: Applications, challenges, and future prospects,” *IEEE Access*, 2025.
- [14] S. L. Choi, R. Jain, C. Feng, P. Emami, H. Zhang, J. Hong, T. Kim, S. Park, F. Ding, M. Baggu *et al.*, “Generative ai for power grid operations,” National Renewable Energy Laboratory (NREL), Golden, CO (United States), Tech. Rep., 2024.
- [15] Q. Chen, S. Bu, H. Wang, and C. Lei, “Real-time multi-stability risk assessment and visualization of power systems: A graph neural network-based method,” *IEEE Transactions on Power Systems*, 2024.
- [16] Y. Zhang, M. Yue, J. Wang, and S. Yoo, “Multi-agent graph-attention deep reinforcement learning for post-contingency grid emergency voltage control,” *IEEE Transactions on Neural Networks and Learning Systems*, vol. 35, no. 3, pp. 3340–3350, 2024.
- [17] K. Wang, W. Wei, T. Xiao, S. Huang, B. Zhou, and H. Diao, “Power system preventive control aided by a graph neural network-based transient security assessment surrogate,” *Energy Reports*, vol. 8, pp. 943–951, 2022.
- [18] V. Balasubramanian, S.-S. Ho, and V. Vovk, *Conformal prediction for reliable machine learning: theory, adaptations and applications*. Newnes, 2014.
- [19] G. Shafer and V. Vovk, “A tutorial on conformal prediction.” *Journal of Machine Learning Research*, vol. 9, no. 3, 2008.
- [20] M. Zaffran, O. Féron, Y. Goude, J. Josse, and A. Dieuleveut, “Adaptive conformal predictions for time series,” in *International Conference on Machine Learning*. PMLR, 2022, pp. 25 834–25 866.
- [21] W. F. Tinney and C. E. Hart, “Power flow solution by newton’s method,” *IEEE Transactions on Power Apparatus and systems*, no. 11, pp. 1449–1460, 1967.
- [22] A. Puech, M. Mazzonelli, C. Cintas, T. R. Govindasamy, M. Mngomezulu, J. Weiss, M. Baù, A. Varbella, F. Mirallès, K. Kim, L. Xie, H. F. Hamann, E. Vos, and T. Brunschwiler, “gridfm-datakit-v1: A python library for scalable and realistic power flow

and optimal power flow data generation,” 2025. [Online]. Available: <https://arxiv.org/abs/2512.14658>